Volume 59
Number 56
18 July 2023
Pages 8607–8748

ChemComm

Chemical Communications

rsc.li/chemcomm

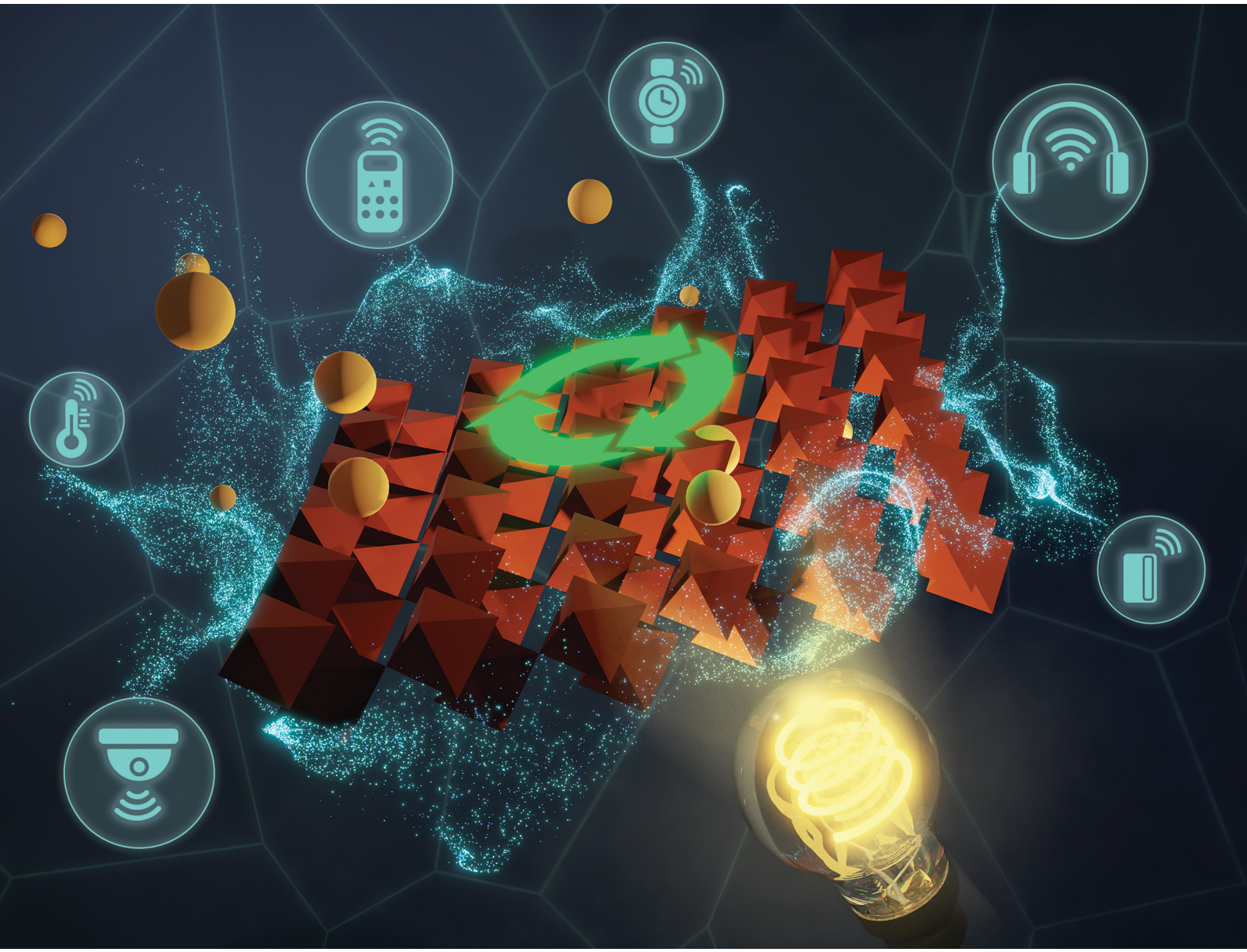

ISSN 1359-7345

ROYAL SOCIETY OF CHEMISTRY

FEATURE ARTICLE

Paola Vivo *et al.*

Lead-free perovskite-inspired semiconductors for indoor light-harvesting – the present and the future

ChemComm

ROYAL SOCIETY OF CHEMISTRY

FEATURE ARTICLE

View Article Online
View Journal | View Issue

Cite this: *Chem. Commun.*, 2023, **59**, 8616

Lead-free perovskite-inspired semiconductors for indoor light-harvesting – the present and the future

G. Krishnamurthy Grandhi,[a] Lethy Krishnan Jagadamma,[b] Vipinraj Sugathan,[a] Basheer Al-Anesi,[a] Debjit Manna[a] and Paola Vivo *[a]

Are lead-free perovskite-inspired materials (PIMs) the wise choice for efficient yet sustainable indoor light harvesting? This feature article outlines how wide-bandgap PIMs can provide a positive answer to this compelling question. The wide band gaps can hinder sunlight absorption, in turn limiting the solar cell performance. However, PIMs based on group VA of the periodic table can theoretically lead to an outstanding indoor power conversion efficiency up to 60% when their band gap is ~2 eV. Yet, the research on PIM-based indoor photovoltaics (IPVs) is still in an early stage with highest indoor device efficiencies up to 10%. This article reviews the recent advancements on PIMs for IPVs and identifies the main limiting factors of device performance, thus suggesting effective strategies to address them. We emphasize the poor operational stability of the IPV devices of PIMs being the key bottleneck for the vast adoption of this technology. We believe that this report can provide a solid scaffolding for further researching this fascinating class of materials, ultimately supporting our vision that, upon extensive advancement of the stability and efficiency, PIMs with wide bandgap will become a contender for the next-generation absorbers for sustainable indoor light harvesting.

Received 17th April 2023,
Accepted 30th May 2023

DOI: 10.1039/d3cc01881d

rsc.li/chemcomm

[a] *Hybrid Solar Cells, Faculty of Engineering and Natural Sciences, Tampere University, P.O. Box 541, FI-33014, Tampere, Finland. E-mail: paola.vivo@tuni.fi*
[b] *Energy Harvesting Research Group, SUPA, School of Physics and Astronomy, University of St Andrews, North Haugh, St Andrews, KY16 9SS, UK*

The urge to self-power the wireless Internet of Things (IoT) ecosystem in a cost-effective and sustainable way has recently led to a growing demand for indoor photovoltaics (IPVs).[1] Among the various emerging IPV technologies, *e.g.*, hydrogenated amorphous silicon (a-Si:H), dye-sensitized solar cells (DSSCs)

G. Krishnamurthy Grandhi

Dr G. Krishnamurthy Grandhi received his PhD in Materials Chemistry from Jawaharlal Nehru Centre for Advanced Scientific Research in 2017. Currently, he is a postdoctoral fellow at Hybrid Solar Cells group at Tampere University. His research interests mainly focus on the synthesis of halide perovskite-based nanocrystals and thin films for optoelectronic applications, particularly indoor photovoltaics.

Lethy Krishnan Jagadamma

Dr Lethy Krishnan Jagadamma is a UKRI-Future Leaders Fellow and leads the Energy Harvesting Research Group at the School of Physics and Astronomy, University of St Andrews. In 2017, she was awarded Marie-Curie Individual Fellowship, to focus her research on the 'Time-resolved photovoltaic properties of hybrid perovskite semiconductors.' In 2020, she was awarded the prestigious UKRI-Future Leaders Fellowship to build her research team. Currently, her research focus is on combining material focussed innovation with that of the emerging huge technologies such as the Internet of Things (IoT) and Wearables to positively contribute to achieving the big target of 'Energy Sustainability.

and organic photovoltaics (OPVs), lead halide perovskites (LHPs) currently hold the record of the highest indoor power conversion efficiency (PCE(i)) exceeding 40% at 1000 lux illuminance.[2] This has been ensured by the defect-tolerance nature of LHPs and their tunable absorption spectra to match those of the typical indoor light spectra. Peng *et al.* calculated the photovoltaic efficiency limits under 1000 lux white light-emitting diode (WLED) illumination as a function of the band gap (Fig. 1a) using the indoor spectroscopically limited maximum efficiency (i-SLME) method.[3] According to this study, a maximum theoretical PCE(i) of ≈60% can be achieved for absorbers with band gaps around 1.9 eV. IPV devices employing LHPs demonstrate very high open-circuit voltage (V_{OC}) values >1 V,[4,5] which minimizes the number of cells to be connected in series to obtain the desired power for IoT applications. Nevertheless, the potential lead (Pb) release from LHP-based IPVs embedded within IoT devices represents a substantial toxicity risk and causes concerns for their recycling.[6,7] Therefore, it is important to develop IPV materials that do not pose any threat to the environment or health during and after the lifecycle of the photovoltaic cells. Low-toxicity tin (Sn)-based perovskites led to PCE(i)s approaching 15%.[8,9] However, Sn-based perovskites possess a few drawbacks, including the air-oxidation of Sn^{2+} to Sn^{4+}.[10,11] Efforts are continuously made to suppress the Sn^{2+} oxidation. Yang *et al.* demonstrated a PCE(i) of 12.81% with a V_{OC} of 0.65 V by incorporating catechin with a hydroxyl functional group (as a doping agent) into Sn-based IPV devices to prevent Sn^{2+} oxidation and improve film morphology.[12] The highest performing (PCE(i) of 17.57% under 1062 lux) Sn perovskite device was achieved *via* interlayer passivation with KSCN-based materials, where K^+ and SCN^- ions passivated both bulk and interface defects.[13] The IPV device retained 80% of the original PCE(i) after 1200 h of

Vipinraj Sugathan

Vipinraj Sugathan has done his PhD under a joint PhD program from Indian Institute of Technology Bombay (IITB) and Nanyang Technological University (NTU), Singapore. Expertise in Perovskite Solar cells, device fabrication and exploration into novel lead-free absorbers materials that can be commercially viable in thin film solar cell applications, he also has commendable contributions in conventional Si solar cell performance analysis, dye-sensitised solar cells, nano-synthesis, Tandem solar cells, etc.

Basheer Al-Anesi

Basheer Al-Anesi obtained a Bachelor's degree in Chemistry from Hodeidah University, Yemen. He then received a Master's degree in Materials Chemistry from the Department of Chemistry, University of Eastern Finland, Finland. Currently, he is a doctoral researcher at the Hybrid Solar Cells group at Tampere University. The focus of his research is the design, synthesis, device fabrication, and characterization of lead-free perovskite-inspired materials for photovoltaic applications.

Debjit Manna

Debjit Manna completed his PhD from the Indian Institute of Technology Bombay, India in 2022. He is now a postdoctoral fellow at the Hybrid Solar Cells group at Tampere University. His research interests focus on the design and synthesis of halide perovskite nanocrystals and perovskite thin films for optoelectronic applications.

Paola Vivo

Paola Vivo is an Associate Professor at Tampere University (TAU). She has worked in the field of solution-processable organic and inorganic semiconductors for emerging photovoltaic technologies for over 15 years. After pursuing her PhD in Chemistry (2010), she received several major grants as Principal Investigator, including the prestigious Academy of Finland Fellowship for post-doctoral research in 2013–2017. She currently leads the Hybrid Solar Cells group (https://research.tuni.fi/hsc/) at the Faculty of Engineering and Natural Sciences at TAU. Her research interests include developing novel materials for solar energy applications, with main emphasis on halide perovskites and perovskite-inspired materials.

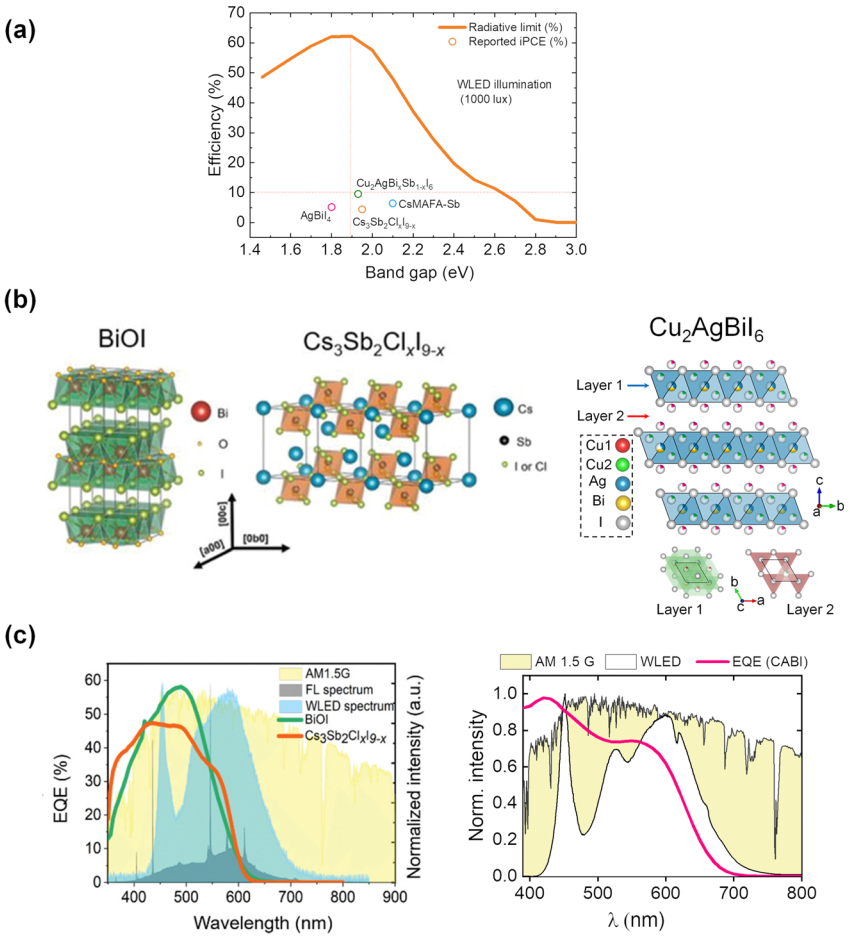

Fig. 1 (a) Radiative-limit (RL) curve (taken from[3]) under indoor lighting conditions as a function of the band gap. The PCE(i) values of PIMs under WLED illumination at 1000 lux are also represented in the same figure. (b) Crystal structures of BiOI and $Cs_3Sb_2(Cl_xI_{9-x})$, adapted from,[3] and CABI (reproduced from[24]). (c) Comparison between the EQE of BiOI and $Cs_3Sb_2Cl_xI_{9-x}$ devices with the WLED, FL, and AM 1.5G spectra (left), reproduced from[3] and the normalized EQE spectrum of a CABI device along with the AM 1.5G and WLED emission (color temperature: 4000 K) spectra (right).

storage in darkness in an inert gas atmosphere. But the stability of Sn-perovskites in air is still not sufficient for any practical application.[12] Furthermore, their typical band gap values (~1.3 V) are much lower than those desired for IPVs (~2 eV).[14] Perovskite-inspired materials (PIMs) comprising air-stable Group VA cations, such as antimony (III) (Sb^{3+}) and bismuth (III) (Bi^{3+}), have recently emerged as promising wide band gap absorbers with low toxicity. The Bi- and Sb-halides and chalcohalides display similar electronic structures as LHPs.[15] Both Sb^{3+} and Bi^{3+} possess the valence electronic configuration of $6s^2$, like Pb^{2+}. In addition to low toxicity,[16] a high dielectric constant of these ions due to their highly polarizable nature may suppress the defect formation probability in the band gap regime.[15,17]

These materials typically crystallize in two-dimensional or layered structures (see the crystal structures of BiOI, $Cs_3Sb_2Cl_xI_{9-x}$, and Cu_2AgBiI_6 (CABI) in Fig. 1b) and own band gaps in the 1.9–2.0 eV range.[3,18] Their adoption as absorbers in single-junction solar cells led to modest efficiencies up to 4%[19] mostly due to their wide band gaps, non-ideal for outdoor sunlight absorption. However, these large band gaps could be beneficial for applications in tandem solar cells and IPVs. This research is in its early infancy with only a handful of examples of PIM-based IPVs (Table 1) and with still no PIM-based tandem cells reported.[18]

Current research and outlook on PIM-based IPVs

As shown in Fig. 1a, the wide band gap values (~2 eV) of PIMs ensure an enhanced photovoltaic performance under indoor *vs.* outdoor lighting conditions. The suitability of the wide band gap PIMs for IPVs can be corroborated by the great match between the external quantum efficiency (EQE) spectra of these materials and the WLED and fluorescence lamp (FL) spectra with respect to the AM 1.5G (1-Sun) spectrum (see Fig. 1c). The PCEs of the photovoltaic devices based on BiOI and $Cs_3Sb_2Cl_xI_{9-x}$ were enhanced from ~1% under 1-Sun to 4–5% under indoor light sources, as demonstrated by Peng *et al.* in their first IPV study on PIMs in 2021.[3] Though both the materials have bandgap values slightly larger than 1.9 eV, the corresponding IPV devices yielded moderate V_{OC} values of

Table 1 Performance of state-of-the-art PIM-based IPVs at 1000 lux illumination

Active layer	Bandgap/type	Device structure	Light source	PCE(i) (%)	FF	J_{sc} (μA cm^{-2})	V_{OC} (V)	Ref.
$Cs_3Sb_2[Cl_xI_{9-x}]$	1.95 eV/near-direct	FTO/TiO_2/m-TiO_2($Cs_3Sb_2Cl_xI_{9-x}$)/Poly-TPD/Au	WLED	4.4	0.40	76	0.47	3
			FL	4.9	0.42	82	0.49	
BiOI	1.93 eV/direct	ITO/NiO_x/BiOI/ZnO/Cr/Ag	WLED	4.0	0.38	56	0.60	3
			FL	4.4	0.40	62	0.60	
$AgBiI_4$	1.8 eV/direct	FTO/c-TiO_2/$AgBiI_4$/spiro-OMeTAD/Au	WLED	5.17	0.56	5.7	0.55	21
$ATBiI_4$ (AT = 2-aminothiazolium)	1.78 eV	FTO/c-TiO_2/$ATBiI_4$/PTAA/Ag	WLED	0.52	0.50	4.35	0.71	23
$Cs_{2.4}MA_{0.5}FA_{0.1}Sb_2I_{8.5}Cl_{0.5}$	2.1 eV/direct	FTO/c-TiO_2/$Cs_{2.4}MA_{0.5}FA_{0.1}Sb_2I_{8.5}Cl_{0.5}$/P3HT/Au	WLED	6.37	0.61	106.7	060	20
Cu_2AgBiI_6 + HI	1.94 eV/direct	FTO/c-TiO_2/Cu_2AgBiI_6 + HI/Spiro-OMeTAD/Au	WLED	4.7	0.65	80	0.60	24
Cu_2AgBiI_6	1.91 eV/direct	FTO/c-TiO_2/m-TiO_2/Cu_2AgBiI_6/Spiro-OMeTAD/Au	WLED	5.52	0.67	72	0.53	25
Sb-alloyed Cu_2AgBiI_6	1.95 eV/direct	FTO/c-TiO_2/m-TiO_2/Cu_2AgBiI_6-Sb/Spiro-OMeTAD/Au	WLED	9.53	0.67	128	0.51	26

0.49 V ($Cs_3Sb_2Cl_xI_{9-x}$) and 0.6 V (BiOI), which accounts for voltage losses of more than 1.3 V. Recently, we developed a triple-cation Sb-based PIM with an elemental composition of $Cs_{2.4}MA_{0.5}FA_{0.1}Sb_2I_{8.5}Cl_{0.5}$, CsMAFA-Sb (band gap ~2 eV). Our design is the first example of hybrid organic–inorganic cation mixing involving Cs, methylammonium (MA), and formamidinium (FA) cations. The corresponding photovoltaic devices delivered a PCE(i) of 6.4% and an improved V_{OC} of 0.6 V at 1000 lux illumination.[20] In this case, the cation mixing reduced the defect density in the Sb-PIM layer of the device.[20] Turkevych *et al.* explored the IPV potential of silver iodobismuthates deposited by co-evaporation.[21] $AgBiI_4$-based devices demonstrated a PCE(i) of 5.17% and a corresponding V_{OC} of 0.55 V under 1000 lux WLED illumination. Replacing the Ag^+ in the above composition with a 2-aminothiazolium (AT) cation, Arivazhagan *et al.*[22] reported $ATBiI_4$ photoactive thin films with a bandgap of 1.78 eV, leading to a corresponding modest PCE(i) of 0.54%. However, these devices displayed relatively high V_{OC} values of 0.71 V under 1000 lux illumination.

The authors attributed this enhanced performance to the reduced trap density and high built-in potential, which suppressed the interfacial charge accumulation.

The quaternary CABI with a band gap of 1.94 eV, first reported by Sansom *et al.*,[18] has been recently investigated by us in IPVs. First, we achieved a PCE(i) of 4.7% and V_{OC} of 0.6 V for CABI-based IPV devices in a planar architecture through microstructure engineering of the CABI absorber layer by hydroiodic acid (HI) additive.[24] More recently, mesoscopic CABI IPV cells delivered a PCE(i) of 5.52% and 5.07% under WLED illuminations of 1000 and 100 lux, respectively.[25] The thickness of the mesoporous titania (mp-TiO_2) layer plays a critical role in maximizing the PCE(i) of the devices through fill factor (FF) and short-circuit current density (J_{SC}) enhancements. Lately, we reported a PCE(i) of ~10% (9.53%) under 1000 lux, *i.e.*, almost double the previous value of 5.52%, for CABI devices upon Bi–Sb co-alloying (CABI-Sb).[26] The efficiency increase was mainly due to the enhancement of J_{SC}. Our CABI-Sb study demonstrates a significant advancement in the performance of PIM-based IPVs, promising a large room for further improvement in PCE(i) through V_{OC} optimization. The CABI-Sb device displayed impressive PCE(i) values of 6.65% and 4.3% even at the low-light WLED intensities of 200 lux and 50 lux, respectively.

Suppressed carrier self-trapping is necessary

Strong electron–phonon coupling in Sb- and Bi-based PIMs leads to the excited-state trapping of charge carriers, thereby reducing their mobility and fundamentally limiting their optoelectronic device performance.[27] Since the charge carrier diffusion lengths in these materials are typically low (≤100 nm)[27,28] and fall within the absorber layer thickness in the photovoltaic devices, the self-trapping induced carrier mobility drop leads to a further reduction in the drift and diffusion lengths, in turn causing J_{SC} and FF losses. The spectroscopic studies predict low carrier mobilities (~1 cm^2 V^{-1} s^{-1}) in Bi- and Sb-based PIMs at room temperature arising from self-trapping mediated charge-carrier localization.[29–31] Rondiya *et al.* summarized the J_{SC} and PCE values of various Bi-based PIM photovoltaic devices, which are all well below their theoretical limits, partially due to the self-trapping nature of the charge carriers.[32] The carrier-trapping process also leads to V_{OC} losses and high dark current generation in PIM-based devices.

The self-trapping can be tuned by modifying the local symmetry of the polyhedra involving carrier-trapping.[33] Recently, we hypothesized the reduction of self-trapping in CABI by the partial alloying of some of the bismuth (III)-sites with antimony (III) ions, which leads to the local symmetry enhancement at the octahedral lattice sites of CABI.[26] However, to unequivocally prove the increase in the number of free carriers in CABI-Sb through the lowering of the number of STEs, advanced studies like optical-pump tera-hertz-probe (OPTP) spectroscopy, should be performed[30,34] The suppressed carrier self-trapping in CABI through Sb alloying enabled a significant enhancement of the J_{SC} value of the corresponding IPV device. Similarly, mixing of the A-site of $Cs_3Sb_2I_9$ with methylammonium and formamidinium ions resulted in a nearly undetectable luminescence signal,[31] unlike the weak self-trapped exciton emission observed for the pristine $Cs_3Sb_2I_9$.[35] The cation mixing remarkably contributed to increase the PCE(i) of Sb-based IPVs from 4.9% to 6.4%.[3,31] These observations suggest that compositional engineering holds a

great promise to alter the symmetry of the lattice points involved in the self-trapped exciton (STE) process and diminish carrier trapping-related non-radiative losses in PIM-based photovoltaic cells. In addition, the compositional engineering was proposed to increase the mobility of charge carriers by reducing their effective masses in Cs_2AgBiX_6 (X = Br, Cl).[36]

Open circuit voltage (V_{OC}) losses should be minimized

The theoretical optimum bandgap for IPVs 1.9–2.0 eV, and the highest predicted V_{OC} is 1.4–1.5 eV.[37,38] However, there are only a few reports on halide perovskite photovoltaics with the experimentally observed V_{OC} of >1 V under indoor lighting conditions (1000 lux).[39,40] Both reports are based on conventional LHP compositions (*i.e.*, $CsPbI_2Br$ and $CH_3NH_3PbI_{2-x}BrCl_x$).

A systematic comparison between the optical bandgap (~1.8–2.0 eV) of the PIMs and their reported V_{OC} values (0.5–0.6 V) under indoor illumination reveals that the PIM compositions suffer a high V_{OC} loss of ~1.3–1.4 V (Fig. 2), which is huge compared to what has been reported for the LHP devices under 1-Sun illumination (less than 0.5 V). A voltage loss of ~0.2 V is expected and systematically observed while comparing the V_{OC} of LHP devices under indoor and 1-Sun illuminations due to the differences in light intensity. To maximise the IPV efficiency of these PIMs, it is essential to reduce the difference between the bandgap and the observed V_{OC}.

Recently, Bahadani[41] has quantified the different energy losses in IPVs considering GaAs and GaInP as test cells and a warm WLED as the illumination source. For all the cases, the highest energy loss was due to the thermalisation losses (30–40%) and to the junction loss (20–30%). However, these cells demonstrated relatively low non-radiative recombination losses (~4 to 8%).

For the photovoltaic devices in general (and specifically for perovskite solar cells), three different voltage loss pathways (due to Shockley–Queisser limit, radiative losses, and Shockley–Read–Hall (SRH)-type losses) have been previously reported.[42–46] Recently, Dong *et al.*[47] have quantified these losses for perovskite solar cells (Cs/FA/MA-LHP) as 273 mV, 3.12 mV, and 250.07 mV (for 1-Sun illumination), respectively. In the case of halide perovskites, the typical trap density of the order of $\sim 10^{15}$ cm^{-3} is comparable to or slightly lower than the typical photogenerated carrier density of $\sim 10^{15}$–10^{16} cm^{-3} under 1-sun illumination.[48] Still, these perovskite solar cells show remarkable efficiencies under low-intensity indoor/solar illumination (trap-dominated regime) because of the defect-tolerant nature of the LHPs or the entirely different charge trapping/de-trapping mechanism in these materials compared to other PV materials.[49]

In the case of Pb-free PIMs, the reported trap density is even higher than that of the halide Pb-based perovskites. Ran *et al.*[50] and Ivaturi *et al.*[23] reported trap densities of 10^{18}–$10^{17}$$cm^{-3}$ for PIM-based films, which are at least one-to-two orders of magnitude higher than those of the Pb-based halide perovskites. The devices with lower trap density showed a higher V_{OC} of 0.8 V under 1-sun illumination. To achieve a high V_{OC} (>1 V) for PIM-based IPVs, one good starting point would be to obtain high V_{OC} under 1-Sun and reduce the voltage losses under indoor lighting conditions. Thus, to maximise the V_{OC} of PIM-based indoor photovoltaics, there should be more investigation to explore the nature and energy of the traps (shallow, or deep), their density distribution as a function of composition, the formation energy required, and the feasible trap reduction methodologies. Fig. 3, adapted from reference[51] shows how reducing the trap density can still retain a high V_{OC} even at low illumination intensities.

However, it is interesting to note that the V_{OC} losses for the best-performing CABI-Sb (PCE(i) = 9.5%) and CsMAFA-Sb (PCE(i) = 6.4%) PIM-based IPV devices are 0.13 V and 0.20 V, respectively when the illumination source changes from 1-Sun to 1000 lux WLED.[26,31] Modest V_{OC} losses of ≈0.2 V have been reported even for high-performing IPVs.[52,53] This suggests that V_{OC} losses due to lowering the light intensity are not very high in the IPV devices of these two materials. However, the low indoor V_{OC} values of just ~0.6 V in these devices are due to already low V_{OC} values achieved under 1-Sun, particularly in the case of CABI.[24–26,28] Hoye and co-workers examined the performance limiting factors of $Cs_2Ag(Sb_xBi_{1-x})Br_6$ solar

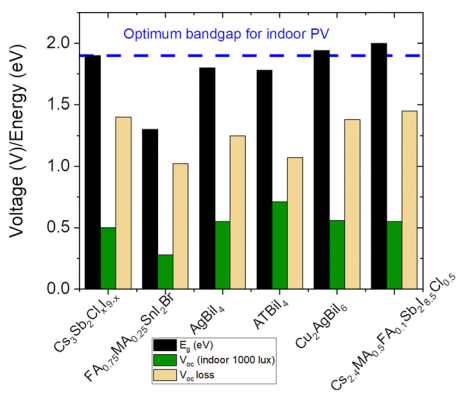

Fig. 2 Optical bandgap, experimentally obtained V_{OC}, and voltage losses of PIM-based IPVs.

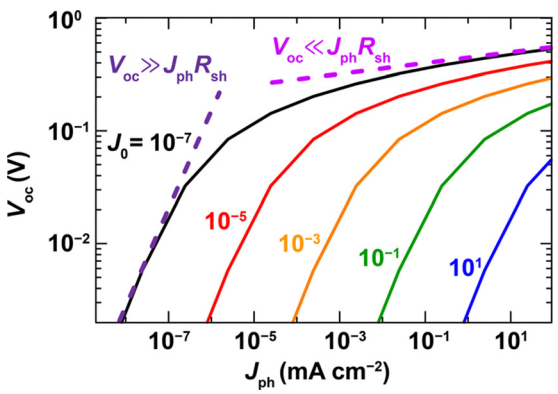

Fig. 3 The simulated graph showing how reducing the leakage current can sustain high photovoltage even under low intensity illumination (adapted from[105]).

cells.[54] They demonstrated that sub-band gap states are accountable for the V_{OC} losses. Similarly, sub-band gap states are detected in CABI;[18] however, their influence on CABI devices is not yet studied. On the other hand, density functional theory calculations have suggested that Sb-alloying in CABI increases the defect or vacancy formation energy.[26] While the co-alloying has nearly doubled the J_{SC} of the CABI IPV devices, it only resulted in very small enhancement in their V_{OC} values. The low V_{OC} values of the devices despite the suppressed intrinsic defect formation and carrier-self trapping could be explained by the non-radiative recombination of the charge carriers at the surface (interfacial recombination) or the grain boundaries (within the bulk) of the CABI layer. Such undesired recombination process may be promoted by the typical sub optimal morphology of CABI,[18,24] which has been so far only partially addressed through additive and compositional engineering strategies.[24,26] Therefore, morphological engineering and surface passivation strategies should be employed, inspired by works on both LHPs[55] and other PIMs,[56–58] to mitigate the V_{OC} losses arising from SRH and interface recombination and push their PCE(i)s towards their theoretical limits of 50–60% (see Fig. 1a). The low V_{OC} values also call for exploring different hole transport and electron transport layers (HTLs and ETLs) than those typically used in LHP-based devices (*e.g.*, Spiro-OMeTAD and P3HT as HTLs; titanium and tin oxides as ETLs), as a good energy level matching is also crucial to achieving high V_{OC}.

Device operational stability needs immediate attention

Lead-free PIM films are usually stable when stored in air owing to the stable oxidation states of Bi^{3+} and Sb^{3+}. For instance, the X-ray diffraction (XRD) patterns of CABI and Sb-PIM collected before and after months of air storage show no changes (see Fig. 4a), indicating their high phase stability. In another study, CABI and $AgBiI_4$ stored in the air displayed no signs of degradation after exposure to solar light for one week.[18] However, long-term stability of corresponding IPV cells is compulsory for their commercial applications. The stability of the photovoltaic cells is expected to be longer under indoor illumination than 1-Sun due to mild operation conditions, such as low-light intensity and no drastic variations in the humidity and light intensity. Commonly, the reported stability of LHP IPV cells has been assessed in terms of shelf-lifetime trends. For instance, Cheng *et al.* demonstrated the long-term stability of triple-anion methylammonium LHP cells with nearly 95% of their original PCE value retained after 2000 h of storage under indoor light.[40] Chen *et al.* reported the longest known shelf-life stability for LHP IPV cells based on a vacuum-deposited LHP layer, which shows a negligible loss in efficiency under continuous exposure to indoor light of intensities between 200 and 1000 lux for 16 months.[59] On the contrary, such long-term stability studies have not been yet reported for PIM-based IPV cells. In addition, to mimic the real-world behavior of the IPV cells, their operational stability should be carefully examined, similarly to the case of LHP solar cells.[60] Among the available standard protocols to assess the operational stability of halide perovskite photovoltaics, maximum power point tracking (MPPT), which monitors the device performance under constant electric load and continuous illumination, sheds light on the intrinsic stability of the devices.[61] As a case study, we report the data related to IPVs employing CABI or triple-cation Sb-based PIM (CsMAFA-Sb). The performance of the unencapsulated devices in air (RH $\approx$ 50%) is monitored at the maximum power point (MPP) under continuous WLED (1000 lux) illumination (see Fig. 4b and c). The CABI IPV cell retains nearly 50% of its original PCE after 120 h of continuous operation. On the other hand, the CsMAFA-Sb device loses 40% of its original PCE already after 7 hours of air exposure. The operational stability of both CABI and CsMAFA-Sb IPVs is poor,[62] which leaves them still far from any practical utilization. This is in contrast with the respectable shelf-lifetime stability of CABI and CsMAFA-Sb films in the air (Fig. 4a).[20,24] These observations exemplify that absorber material stability does not guarantee the corresponding device stability. In addition, the CABI device degrades more rapidly under 1-Sun (Fig. 4d) compared to the WLED illumination. This hints at the accelerated degradation of the device under high-light intensity illumination.

The degradation mechanisms of the photovoltaic devices of LHPs under 1-Sun illumination are widely studied and quite well-established.[60] One of the common degradation mechanisms in the LHP devices, as far as the absorber layer is concerned, is the ion migration under electric bias and illumination.[60,63] Recently, Kulkarni *et al.* demonstrated that vacancy or defect-induced ion migration is a major degradation pathway of the Ag-Bi-I PIM-based solar cells under ambient storage.[64] This could be a plausible degradation pathway in many wide-bandgap PIMs as they often comprise a large number of defects.[65] However, further research should be performed to understand the underlying causes of the degradation in PIM-based photovoltaic cells under 1-Sun and indoor illuminations. In addition, effective strategies should be applied to extend the device lifetime of PIMs. Li *et al.* summarized the literature on various efficient strategies, which involve charged defect passivation, compositional tuning, surface passivation by organic and inorganic layers, and so on, to improve the operational stability of the LHP solar cells.[60] Although the optoelectronic behaviour of PIMs differs from LHPs, a good starting point may be to explore some of the strategies mentioned by Li *et al.*, which may also improve the V_{OC} values and other device parameters.

Prospect IPV absorbers

To address the above-mentioned instability and toxicity concerns of LHPs, the development of novel, and inherently more stable, PIMs has been the focus of recent research. Yet, more efforts are required to expand the library of potential non-toxic IPV absorbers. The following PIM candidates for IPVs are proposed based on (i) suitability of band gaps (1.9–2.0 eV) for

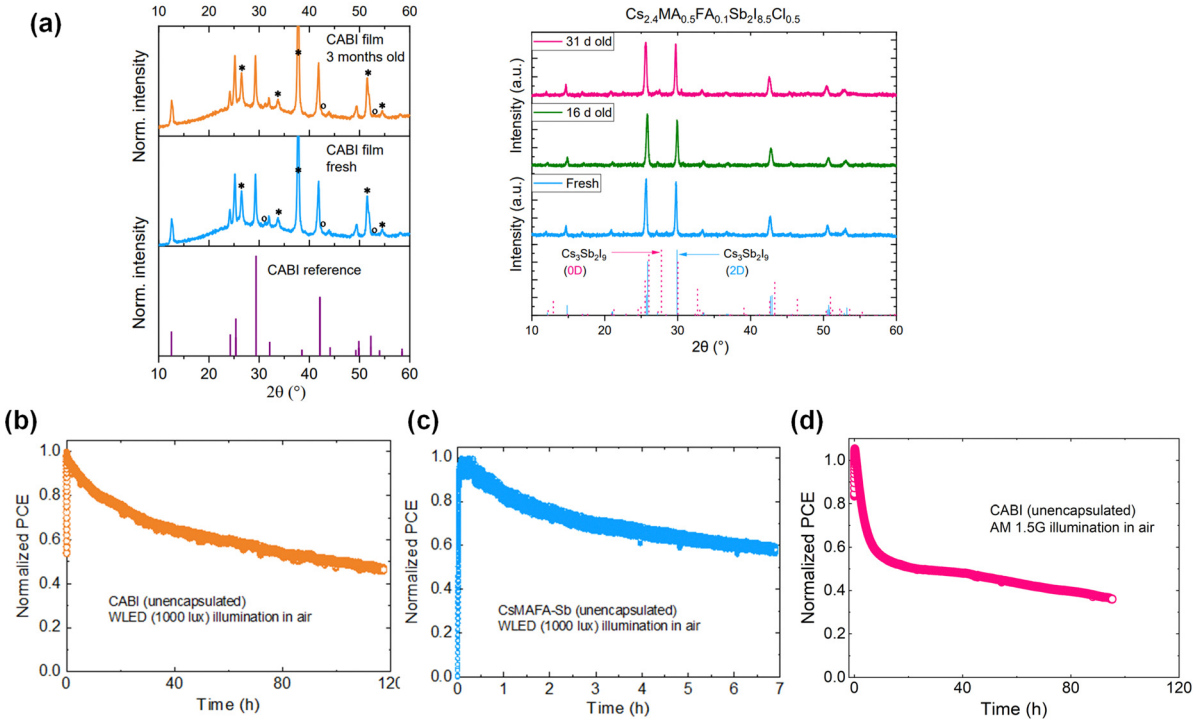

Fig. 4 (a) XRD patterns of fresh and aged CABI films stored in air (reproduced from[24]) and fresh and aged CsMAFA-Sb films stored in dry air (RH of 15%) (reproduced from[31]). MPP tracking of unencapsulated devices (in their n–i–p planar device architecture) of (b) CABI and (c) CsMAFA-Sb under WLED (1000 lux) illumination, and (d) CABI under 1-Sun illumination in air (RH ~50%).

indoor light-harvesting, (ii) reasonable PCEs under 1-Sun, (iii) optoelectronic properties suitable for photovoltaic applications, (iv) high defect-tolerance, and (v) air-stability.

Three-dimensional (3D) materials

Cesium germanium iodide ($CsGeI_3$), with a band gap of ~1.89 eV, has been explored for solar cell applications, yielding a PCE of 4.94%. This is one of the most efficient photovoltaic absorbers among the Pb-free perovskite structures.[66] Ba_2AgIO_6, a low-temperature processable oxide analogue of halide perovskites, is another stable and encouraging alternative with a band gap (1.9 eV) close to the ideal value required for IPV absorbers.[67]

3D $MASbSI_2$ (band gap = 2.03 eV) was recently found suitable for photovoltaic applications (PCE = 3.08%).[68]

Two-dimensional (2D) materials

$PEA_2(Ge/Sn)I_4$ possesses a band gaps around 2.1–2.2 eV.[69,70] These are the candidates with the highest PCEs under 1-Sun when considering wide band gap materials ideal for IPV applications. For example, $(PEA)_2GeI_4$ exhibits luminescence at room temperature with a moderate lifetime, showing promise for photovoltaic applications. Another popular family of compounds, $A_3(Sb/Bi)_2X_9$, with bandgaps in the 1.9–2.1 eV range is also not much explored for IPV applications and can be a great prospect considering their favaourable optoelectronic properties.[71–74] Among these, $MA_3Sb_2I_{9-x}Cl_x$ (band gap = 2.2 eV) yielded a PCE of 3.34% under 1-Sun,[75] which makes it a potential IPV absorber. Sb–Bi co-alloying in these materials may favourably modify their optoelectronic properties, as in the case of CABI. Other 2D candidates for consideration can be MA_2PdCl_4 (band gap = 2.2 eV) and $CsBi_3I_{10}$ (band gap = 1.8 eV).[76]

Double perovskites and vacancy-ordered double perovskites, $A_2Ag(Sb/Bi)X_6$ (A = Cs and MA; X = Br and Cl), having bandgap tunability over a wide range (1.6–2.6 eV), offer great potential as candidates that remain unexplored for IPV applications.[77–82] The double perovskite $Cs_2AgBiBr_6$, with a PCE of 2.8% and bandgap around 2.2 eV, is the most explored PIM when it comes to solar cells.[83] Additionally, the high air-stability and the earth abundant nature of the ivolved elements make $Cs_2AgBiBr_6$ ideal candidates for IPV applications. Cs_2TiBr_6 (band gap = 1.8 eV), a vacancy-double perovskite with a reported PCE (1-Sun) of ≈ 3.3%, is also a potential IPV absorber.[84,85] Cs_2PdX_6, with tunable band gaps over the 1.6–2.22 eV range by halide compositional engineering, are suitable for different indoor light environments.[86,87]

Although the IPV performance of a silver iodobismuthate with the composition of $AgBiI_4$ has been already examined,[21] another member of the same family, Ag_3BiI_6 that yielded PCE values up to 4.2–5.4% (and notable J_{SC} and FF) under 1-Sun due to improved charge transport[88] may ensure >10% IPV efficiencies. Antimony sulfoiodide (SbSI) with a band gap of ≈ 2.2 eV, high defect-tolerance (dielectric constant in the order of 10^4), and high stability offers a great promise for IPV applications.[89] The IPV performance of BiOI, a deep-trap tolerant,[90] can be further improved if the morphology-related limitations are addressed.[91]

Furthermore, we believe that the compositional engineering with the introduction of organic cations such as methylammonium (MA) and formadinimium (FA), by increasing the overall dielectric constant of the material, may improve the defect tolerance by reducing the capture cross-section of the charged defects.[31,92] In addition to the materials listed so far, air-stable, wide band gap chalcogenide perovskites with tuneable band gaps of 1.73–2.87 eV[93] can be worth investigating for their IPV performance. Preliminary DFT calculations suggest that $BaZrS_3$ (band gap $\sim$ 1.8 eV) is defect-tolerant, similarly to LHPs.[94] Low-temperature processing of high-quality chalcogenide perovskite films must be established to realize their full commercialisation potential.

Recently there has been much interest in the application of machine learning (ML) in hybrid perovskite solar cells for screening novel compositions, optimising the fabrication processes, and developing more stable compositions.[95,96] While designing novel compositions of perovskite-inspired Pb-free materials, the available materials parameters of the corresponding Pb-containing perovskites can provide the desirable input ML parameters required for the optimisation.[97] This would reduce the initial stages of experimentation for the implementation of ML. Even though there are no reports yet demonstrating the use of ML in optimising IPVs, the same design principles developed for the LHP solar cells can be extended to the perovskite IPVs as well, upon appropriate modifications in the input data set. Since there are numerous available publications on the bandgap tuning of halide perovskites, their electrical properties, crystal structure, thin film fabrication *etc.*, the 'data preparation' stage of the ML workflow is relatively straightforward.[98] The application of ML in indoor PV has the potential to boost the efficiency towards the theoretical limit of 50–60% by rapid material design, discovery, and PV property evaluation.

By combining the unique strengths of high throughput synthesis and ML, recently Sun *et al.*[99] have discovered 75 PIM compositions in just 2 months, which are suitable for energy harvesting applications. A few dozens of Pb-free PIMs were also discovered in an accelerated matter, which allowed avoiding the slow incremental trial and error method. The most impressive aspect was the development of four compounds and 18 alloy compositions of Pb-free perovskite-inspired compositions in the thin film form, which otherwise existed only in the crystal bulk form, in turn enabling their adoption in many thin film architecture optoelectronic devices.

In addition to the material screening for the photovoltaic applications,[1,100] the suitability of artificial intelligence in predicting the stability, and the reap, rest, and recovery (3R) of halide perovskites has been also reported and may applied also to PIM-based IPVs to boost their credibility for future practical applications.[101]

In conclusion, PIMs have had a promising start for IPVs. Their low V_{OC} values of $\sim$0.5–0.6 V remain the major drawback restricting them from reaching PCE(i) values beyond 10% and towards their theoretical limits. The wide band gap nature and typical sub optimal morphology of PIMs typically lead to dominant non-radiative recombination both in their bulk and at their surface or interfaces. Our studies on CsMAFA-Sb and CABI-Sb indicate that cation co-alloying is a promising strategy to improve the defect tolerance of PIMs. We believe that the combination of compositional engineering and microstructure enhancement is the key to significantly boosting the efficiency of lead-free perovskite-inspired IPVs. In all the PIM-based IPV studies, the champion devices under 1-Sun are typically examined under indoor lighting. However, it has been realized in LHPs that the best solar cell performance does not necessarily guarantee the highest indoor device performance.[102,103] Therefore, parameters such as absorber layer thickness, type of charge transport layers, and device architecture should be separately optimized for the PIM-based devices under indoor illumination.

Expanding the library of IPV absorbers by combined computational and experimental methods helps in two ways. Firstly, it helps identifying highly promising candidates. Secondly, it provides a general understanding of the behavior of PIMs under low-light intensities, which will help in modifying the existing IPV materials and rationalize the design of new absorbers. Materials with high defect-tolerance and long diffusion lengths can be discovered through experimental characterizations and ML calculations. In addition to the band gap requirements, the next-generation IPV absorbers should preferably comprise low-toxic and earth-abundant elements. Absorbers with low exciton binding energies, high thermodynamic stabilities, and direct band gap absorption will be promising. Moreover, the absorbers should be solution-processed at low temperatures for cost-effectiveness, large-scale fabrication, and deposition on flexible substrates. The morphology of the PIM-based thin films is far inferior to that of LHPs in terms of both grain size and smoothness. Despite the constant efforts to improve the microstructural properties of PIMs through solution- and vacuum-based methods engaging numerous modifications (*e.g.*, solvent engineering, additives, doping, temperature tuning, and post-annealing treatments), the thin films are often non-continuous (incomplete coverage) and contain significantly large pin holes, which create shunt pathways that cause undesired non-radiative recombination during the IPV device operation. Studies focusing on the understanding of the film crystallization kinetics of the PIMs should be carried out to identify the factors affecting the crystal growth and determine the nucleation mechanisms, which, in turn, will enable high-quality PIM-based thin films. In addition to electronic structure examination, deep crystal structural analysis is also necessary. For instance, the deep trap formation in BiOI is restricted due to its long Bi–I bonds. Furthermore, the band gap requirement may not be strictly applicable in all the cases. For example, despite the low band gap of 1.4 eV of a quaternary chalcogenide halide, $Sn_2SbS_2I_3$, its strong absorption in the 400–650 nm range,[104] where the emission intensities of WLEDs are the highest, may still allow their IPV devices perform efficiently. The PIMs show poor device stability in stark contrast to their high material stability in the air. In addition to the simple monitoring of the shelf-life stability of the devices,

MPPT and other standard operational stability characterizations (*e.g.*, accelerated indoor testing involving day-night cycles) should be widely adopted to demonstrate the potential of PIM-based devices towards commercialization. Therefore, regardless of their performance, an enhanced stability will be even more crucial for the future of PIM-based IPVs. Although the PIMs typically consist of low-toxicity elements, we strongly encourage the research community to investigate the practicality of the IPV devices from a life-cycle perspective. The cradle-to-grave life-cycle assessment of IPVs will provide insights on the energy payback time and the impact of the devices on the environment, which are important parameters in the context of the global PV market. Overall, enhancing the long-term operational stability and efficiency of the PIM-based photovoltaic devices under indoor illumination will lead us closer to the goal of cost-effective, low-toxic, and high-performance IPVs for indoor-located, self-powered IoT devices.

Conflicts of interest

There are no conflicts to declare.

Acknowledgements

The authors thank Miss. Noora Lamminen for the support with the maximum power point data. G. K. G. thanks Tampere Institute for Advanced Study for the postdoctoral funding. P. V. and V. S. acknowledge the financial support of Jane and Aatos Erkko foundation (SOL-TECH project) and Academy of Finland (Decision No. 347772). B.A-A. thanks Vilho, Yrjö and Kalle Väisälä Fund of the Finnish Academy of Science and Letters for the financial support. This work is part of the Academy of Finland Flagship Programme, Photonics Research and Innovation (PREIN), Decision No. 320165.

References

1 I. Mathews, S. N. Kantareddy, T. Buonassisi and I. M. Peters, *Joule*, 2019, **3**, 1415–1426.
2 C. Dong, X. Li, C. Ma, W. Yang, J. Cao, F. Igbari, Z. Wang and L. Liao, *Adv. Funct. Mater.*, 2021, **31**, 2011242.
3 Y. Peng, T. N. Huq, J. Mei, L. Portilla, R. A. Jagt, L. G. Occhipinti, J. L. Macmanus-driscoll, R. L. Z. Hoye and V. Pecunia, *Adv. Energy Mater.*, 2020, **11**, 2002761.
4 Z. Guo, A. K. Jena, I. Takei, G. M. Kim, M. A. Kamarudin, Y. Sanehira, A. Ishii, Y. Numata, S. Hayase and T. Miyasaka, *J. Am. Chem. Soc.*, 2020, **142**, 9725–9734.
5 Z. Guo, S. Zhao, N. Shibayama, A. Kumar Jena, I. Takei and T. Miyasaka, *Adv. Funct. Mater.*, 2022, **32**, 2207554.
6 H. Needleman, *Annu. Rev. Med.*, 2004, **55**, 209–222.
7 J. Li, H.-L. Cao, W.-B. Jiao, Q. Wang, M. Wei, I. Cantone, J. Lü and A. Abate, *Nat. Commun.*, 2020, **11**, 1–5.
8 W. F. Yang, J. J. Cao, C. Dong, M. Li, Q. S. Tian, Z. K. Wang and L. S. Liao, *Appl. Phys. Lett.*, 2021, **118**, 023501.
9 W. F. Yang, J. J. Cao, J. Chen, K. L. Wang, C. Dong, Z. K. Wang and L. S. Liao, *Solar RRL*, 2021, **5**, 1–7.
10 W. Ke, C. C. Stoumpos and M. G. Kanatzidis, *Adv. Mater.*, 2021, **31**, 1803230.
11 J. Cao and F. Yan, *Energy Environ. Sci.*, 2021, **14**, 1286.
12 W. F. Yang, J. J. Cao, C. Dong, M. Li, Q. S. Tian, Z. K. Wang and L. S. Liao, *Appl. Phys. Lett.*, 2021, **118**, 023501.
13 J.-J. Cao, Y.-H. Lou, W.-F. Yang, K.-L. Wang, Z.-H. Su, J. Chen, C.-H. Chen, C. Dong, X.-Y. Gao and Z.-K. Wang, *Chem. Eng. J.*, 2022, **433**, 133832.
14 K. Ruhle and M. Kasemann, Photovoltaic Specialists Conference (PVSC) IEEE 39th, 2013, 2651–2654.
15 R. E. Brandt, V. Stevanović, D. S. Ginley and T. Buonassisi, *MRS Commun.*, 2015, **5**, 265–275.
16 R. Mohan, *Nat. Chem.*, 2010, **2**, 336.
17 L. C. Lee, T. N. Huq, J. L. MacManus-Driscoll and R. L. Z. Hoye, *APL Mater.*, 2018, **6**, 84502.
18 H. C. Sansom, G. Longo, A. D. Wright, L. R. V. Buizza, S. Mahesh, B. Wenger, M. Zanella, M. Abdi-Jalebi, M. J. Pitcher and M. S. Dyer, *J. Am. Chem. Soc.*, 2021, **143**, 3983–3992.
19 I. Turkevych, S. Kazaoui, E. Ito, T. Urano, K. Yamada, H. Tomiyasu, H. Yamagishi, M. Kondo and S. Aramaki, *ChemSusChem*, 2017, **10**, 3754–3759.
20 N. Lamminen, G. K. Grandhi, F. Fasulo, A. Hiltunen, H. Pasanen, M. Liu, B. Al-Anesi, A. Efimov, H. Ali-Löytty, K. Lahtonen, P. Mäkinen, A. Matuhina, A. B. Muñoz-García, M. Pavone and P. Vivo, *Adv. Energy Mater.*, 2022, **13**, 2203175.
21 I. Turkevych, S. Kazaoui, N. Shirakawa and N. Fukuda, *Jpn. J. Appl. Phys.*, 2021, **60**, 2–6.
22 V. Arivazhagan, F. Gun, R. K. K. Reddy, T. Li, M. Adelt, N. Robertson, Y. Chen and A. Ivaturi, *Sustainable Energy Fuels*, 2022, **6**, 3179–3186.
23 V. Arivazhagan, F. Gun, R. K. K. Reddy, T. Li, M. Adelt, N. Robertson, Y. Chen and A. Ivaturi, *Sustainable Energy Fuels*, 2022, **6**, 3179–3186.
24 G. K. Grandhi, B. Al-Anesi, H. Pasanen, H. Ali-Löytty, K. Lahtonen, S. Granroth, N. Christian, A. Matuhina, M. Liu, A. Berdin, V. Pecunia and P. Vivo, *Small*, 2022, **18**, 2203768.
25 G. K. Grandhi, S. Toikkonen, B. Al-Anesi, V. Pecunia and P. Vivo, *Sustainable Energy Fuels*, 2022, **7**, 66–73.
26 B. Al-Anesi, G. K. Grandhi, A. Pecoraro, V. Sugathan, N. S. M. Viswanath, H. Ali-Löytty, M. Liu, T.-P. Ruoko, K. Lahtonen, D. Manna, S. Toikkonen, A. B. Muñoz-García, M. Pavone and P. Vivo, *ChemRxiv*, 2023, preprint, DOI: 10.26434/chemrxiv-2023-nb5jj.
27 B. Wu, W. Ning, Q. Xu, M. Manjappa, M. Feng, S. Ye, J. Fu, S. Lie, T. Yin and F. Wang, *Sci. Adv.*, 2021, **7**, eabd3160.
28 N. Pai, M. Chatti, S. O. Fürer, A. D. Scully, S. R. Raga, N. Rai, B. Tan, A. S. R. Chesman, Z. Xu, K. J. Rietwyk, S. S. Reddy, Y. Hora, G. A. Sepalage, N. Glück, M. Lira-Cantú, U. Bach and A. N. Simonov, *Adv. Energy Mater.*, 2022, 2201482.
29 A. D. Wright, L. R. V. Buizza, K. J. Savill, G. Longo, H. J. Snaith, M. B. Johnston and L. M. Herz, *J. Phys. Chem. Lett.*, 2021, **12**, 3352–3360.
30 L. R. V. Buizza, A. D. Wright, G. Longo, H. C. Sansom, C. Q. Xia, M. J. Rosseinsky, M. B. Johnston, H. J. Snaith and L. M. Herz, *ACS Energy Lett.*, 2021, **6**, 1729–1739.
31 N. Lamminen, G. K. Grandhi, F. Fasulo, A. Hiltunen, H. Pasanen, M. Liu, B. Al-Anesi, A. Efimov, H. Ali-Löytty and K. Lahtonen, *Adv. Energy Mater.*, 2023, **13**, 2203175.
32 S. R. Rondiya, R. A. Jagt, J. L. MacManus-Driscoll, A. Walsh and R. L. Z. Hoye, *Appl. Phys. Lett.*, 2021, **119**, 220501.
33 B. Luo, D. Liang, S. Sun, Y. Xiao, X. Lian, X. Li, M.-D. Li, X.-C. Huang and J. Z. Zhang, *J. Phys. Chem. Lett.*, 2019, **11**, 199–205.
34 L. R. V. Buizza and L. M. Herz, *Adv. Mater.*, 2021, **33**, 2007057.
35 A. Hiltunen, N. Lamminen, H. Salonen, M. Liu and P. Vivo, *Sustainable Energy Fuels*, 2022, **6**, 217–222.
36 J. Leveillee, G. Volonakis and F. Giustino, *J. Phys. Chem. Lett.*, 2021, **12**, 4474–4482.
37 M. Freunek, M. Freunek and L. M. Reindl, *IEEE J. Photovolt.*, 2012, **3**, 59–64.
38 J. K. W. Ho, H. Yin and S. K. So, *J. Mater. Chem. A*, 2020, **8**, 1717–1723.
39 S. Jiang, Y. Bai, Z. Xu, F. Wang, L. Xia, Y. Yang, C. Li and Z. Tan, *Small Methods*, 2022, **6**, 1–9.
40 R. Cheng, C. Chung, H. Zhang, F. Liu, W. Wang, Z. Zhou, S. Wang, A. B. Djurišić and S. Feng, *Adv. Energy Mater.*, 2019, **9**, 1901980.
41 B. H. Hamadani, *Appl. Phys. Lett.*, 2020, **117**, 043904.
42 M. Azzouzi, T. Kirchartz and J. Nelson, *Trends Chem.*, 2019, **1**, 49–62.
43 C. Dong, J. Chen, C. H. Chen, Y. R. Shi, W. F. Yang, K. L. Wang, Z. K. Wang and L. S. Liao, *Nano Energy*, 2022, **94**, 106866.

44 J. Liu, S. Chen, D. Qian, B. Gautam, G. Yang, J. Zhao, J. Bergqvist, F. Zhang, W. Ma, H. Ade, O. Inganäs, K. Gundogdu, F. Gao and H. Yan, *Nat. Energy*, 2016, **1**, 1–48.
45 T. Kirchartz, P. Kaienburg and D. Baran, *J. Phys. Chem. C*, 2018, **122**, 5829–5843.
46 L. Krückemeier, U. Rau, M. Stolterfoht and T. Kirchartz, *Adv. Energy Mater.*, 2020, **10**, 1902573.
47 C. Dong, J. Chen, C. H. Chen, Y. R. Shi, W. F. Yang, K. L. Wang, Z. K. Wang and L. S. Liao, *Nano Energy*, 2022, **94**, 106866.
48 J. M. Richter, M. Abdi-Jalebi, A. Sadhanala, M. Tabachnyk, J. P. H. Rivett, L. M. Pazos-Outón, K. C. Gödel, M. Price, F. Deschler and R. H. Friend, *Nat. Commun.*, 2016, 7.
49 S. D. Stranks, *ACS Energy Lett.*, 2017, **2**, 1515–1525.
50 C. Ran, Z. Wu, J. Xi, F. Yuan, H. Dong, T. Lei, X. He and X. Hou, *J. Phys. Chem. Lett.*, 2017, **8**, 394–400.
51 S. Hwang and T. Yasuda, *Polym. J.*, 2023, **55**, 297.
52 H. Yin, J. K. W. Ho, S. H. Cheung, R. J. Yan, K. L. Chiu, X. Hao and S. K. So, *J. Mater. Chem A*, 2018, **6**, 8579–8585.
53 Y. Cui, Y. Wang, J. Bergqvist, H. Yao, Y. Xu, B. Gao, C. Yang, S. Zhang, O. Inganäs and F. Gao, *Nat. Energy*, 2019, **4**, 768–775.
54 Z. Li, Y.-T. Huang, L. Mohan, S. J. Zelewski, R. H. Friend, J. Briscoe and R. L. Z. Hoye, *Solar RRL*, 2022, **6**, 2200749.
55 Z. Guo, A. K. Jena, G. M. Kim and T. Miyasaka, *Energy Environ. Sci.*, 2022, **15**, 3171–3222.
56 Q. Zhang, C. Wu, X. Qi, F. Lv, Z. Zhang, Y. Liu, S. Wang, B. Qu, Z. Chen and L. Xiao, *ACS Appl. Energy Mater.*, 2019, **2**, 3651–3656.
57 Y. Guo, J. Zhou, F. Zhao, Y. Wu, J. Tao, S. Zuo, J. Jiang, Z. Hu and J. Chu, *Nano Energy*, 2021, **88**, 106281.
58 J. Li, J. Duan, J. Du, X. Yang, Y. Wang, P. Yang, Y. Duan and Q. Tang, *ACS Appl. Mater. Interfaces*, 2020, **12**, 47408–47415.
59 C.-Y. Chen, W.-H. Lee, S.-Y. Hsiao, W.-L. Tsai, L. Yang, H.-L. Lin, H.-J. Chou and H.-W. Lin, *J. Mater. Chem. A*, 2019, **7**, 3612–3617.
60 N. Li, X. Niu, Q. Chen and H. Zhou, *Chem. Soc. Rev.*, 2020, **49**, 8235–8286.
61 M. V. Khenkin, E. A. Katz, A. Abate, G. Bardizza, J. J. Berry, C. Brabec, F. Brunetti, V. Bulović, Q. Burlingame and A. Di Carlo, *Nat. Energy*, 2020, **5**, 35–49.
62 G. Li, Z. Su, L. Canil, D. Hughes, M. H. Aldamasy, J. Dagar, S. Trofimov, L. Wang, W. Zuo and J. J. Jerónimo-Rendon, *Science*, 1979, **2023**(379), 399–403.
63 Y. Yuan and J. Huang, *Acc. Chem. Res.*, 2016, **49**, 286–293.
64 A. Kulkarni, F. Ünlü, N. Pant, J. Kaur, C. Bohr, A. K. Jena, S. Öz, M. Yanagida, Y. Shirai and M. Ikegami, *Solar RRL*, 2021, **5**, 2100077.
65 A. M. Ganose, D. O. Scanlon, A. Walsh and R. L. Z. Hoye, *Nat. Commun.*, 2022, **13**, 1–4.
66 L.-J. Chen, *RSC. Adv.*, 2018, **8**, 18396–18399.
67 G. Volonakis, N. Sakai, H. J. Snaith and F. Giustino, *J. Phys. Chem. Lett.*, 2019, **10**, 1722–1728.
68 R. Nie, A. Mehta, B. Park, H.-W. Kwon, J. Im and S. Il Seok, *J. Am. Chem. Soc.*, 2018, **140**, 872–875.
69 P. Cheng, T. Wu, J. Zhang, Y. Li, J. Liu, L. Jiang, X. Mao, R.-F. Lu, W.-Q. Deng and K. Han, *J. Phys. Chem. Lett.*, 2017, **8**, 4402–4406.
70 Z. Xu, D. B. Mitzi, C. D. Dimitrakopoulos and K. R. Maxcy, *Inorg. Chem.*, 2003, **42**, 2031–2039.
71 C. Zuo and L. Ding, *Angew. Chem.*, 2017, **129**, 6628–6632.
72 C. W. M. Timmermans, S. O. Cholakh and G. Blasse, *J. Solid State Chem.*, 1983, **46**, 222–233.
73 A. J. Lehner, D. H. Fabini, H. A. Evans, C.-A. Hébert, S. R. Smock, J. Hu, H. Wang, J. W. Zwanziger, M. L. Chabinyc and R. Seshadri, *Chem. Mater.*, 2015, **27**, 7137–7148.
74 S. Sun, N. T. P. Hartono, Z. D. Ren, F. Oviedo, A. M. Buscemi, M. Layurova, D. X. Chen, T. Ogunfunmi, J. Thapa and S. Ramasamy, *Joule*, 2019, **3**, 1437–1451.
75 Y. Yang, C. Liu, M. Cai, Y. Liao, Y. Ding, S. Ma, X. Liu, M. Guli, S. Dai and M. K. Nazeeruddin, *ACS Appl. Mater. Interfaces*, 2020, **12**, 17062–17069.
76 G.-X. Liang, X.-Y. Chen, Z.-H. Chen, H.-B. Lan, Z.-H. Zheng, P. Fan, X.-Q. Tian, J.-Y. Duan, Y.-D. Wei and Z.-H. Su, *J. Phys. Chem. C*, 2019, **123**, 27423–27428.
77 A. H. Slavney, T. Hu, A. M. Lindenberg and H. I. Karunadasa, *J. Am. Chem. Soc.*, 2016, **138**, 2138–2141.
78 F. Wei, Z. Deng, S. Sun, F. Zhang, D. M. Evans, G. Kieslich, S. Tominaka, M. A. Carpenter, J. Zhang and P. D. Bristowe, *Chem. Mater.*, 2017, **29**, 1089–1094.
79 E. T. McClure, M. R. Ball, W. Windl and P. M. Woodward, *Chem. Mater.*, 2016, **28**, 1348–1354.
80 F. Wei, Z. Deng, S. Sun, N. T. P. Hartono, H. L. Seng, T. Buonassisi, P. D. Bristowe and A. K. Cheetham, *Chem. Commun.*, 2019, **55**, 3721–3724.
81 J. Kangsabanik, V. Sugathan, A. Yadav, A. Yella and A. Alam, *Phys. Rev. Mater.*, 2018, **2**, 55401.
82 V. Sugathan, J. Kangsabanik, A. Alam and A. Yella, *Energy Fuels*, 2022, **36**, 11100–11107.
83 X. Yang, Y. Chen, P. Liu, H. Xiang, W. Wang, R. Ran, W. Zhou and Z. Shao, *Adv. Funct. Mater.*, 2020, **30**, 2001557.
84 W. Zhang, K. Tao, C. Ji, Z. Sun, S. Han, J. Zhang, Z. Wu and J. Luo, *Inorg. Chem.*, 2018, **57**, 4239–4243.
85 M. Chen, M.-G. Ju, A. D. Carl, Y. Zong, R. L. Grimm, J. Gu, X. C. Zeng, Y. Zhou and N. P. Padture, *Joule*, 2018, **2**, 558–570.
86 N. Sakai, A. A. Haghighirad, M. R. Filip, P. K. Nayak, S. Nayak, A. Ramadan, Z. Wang, F. Giustino and H. J. Snaith, *J. Am. Chem. Soc.*, 2017, **139**, 6030–6033.
87 T. J. Huang, Z. X. Thiang, X. Yin, C. Tang, G. Qi and H. Gong, *Chem. – Eur. J.*, 2016, **22**, 2146–2152.
88 N. Pai, J. Lu, T. R. Gengenbach, A. Seeber, A. S. R. Chesman, L. Jiang, D. C. Senevirathna, P. C. Andrews, U. Bach and Y. Cheng, *Adv. Energy Mater.*, 2019, **9**, 1803396.
89 R. Nie, H. Yun, M. Paik, A. Mehta, B. Park, Y. C. Choi and S. Il Seok, *Adv. Energy Mater.*, 2018, **8**, 1701901.
90 T. N. Huq, L. C. Lee, L. Eyre, W. Li, R. A. Jagt, C. Kim, S. Fearn, V. Pecunia, F. Deschler and J. L. MacManus-Driscoll, *Adv. Funct. Mater.*, 2020, **30**, 1909983.
91 R. L. Z. Hoye, L. C. Lee, R. C. Kurchin, T. N. Huq, K. H. L. Zhang, M. Sponseller, L. Nienhaus, R. E. Brandt, J. Jean and J. A. Polizzotti, *Adv. Mater.*, 2017, **29**, 1702176.
92 R. C. Kurchin, P. Gorai, T. Buonassisi and V. Stevanovic, *Chem. Mater.*, 2018, **30**, 5583–5592.
93 S. Perera, H. Hui, C. Zhao, H. Xue, F. Sun, C. Deng, N. Gross, C. Milleville, X. Xu and D. F. Watson, *Nano Energy*, 2016, **22**, 129–135.
94 X. Wu, W. Gao, J. Chai, C. Ming, M. Chen, H. Zeng, P. Zhang, S. Zhang and Y.-Y. Sun, *Sci. China Mater.*, 2021, **64**, 2976–2986.
95 Y. Liu, X. Tan, J. Liang, H. Han, P. Xiang and W. Yan, *Adv. Funct. Mater.*, 2023, 2214271.
96 Q. Tao, P. Xu, M. Li and W. Lu, *NPJ Comput. Mater.*, 2021, **7**, 1–18.
97 A. Mannodi-Kanakkithodi and M. K. Y. Chan, *Energy Environ. Sci.*, 2022, 1930–1949.
98 Q. Tao, P. Xu, M. Li and W. Lu, *NPJ Comput. Mater.*, 2021, **7**, 1–18.
99 S. Sun, N. T. P. Hartono, Z. D. Ren, F. Oviedo, A. M. Buscemi, M. Layurova, D. X. Chen, T. Ogunfunmi, J. Thapa, S. Ramasamy, C. Settens, B. L. DeCost, A. G. Kusne, Z. Liu, S. I. P. Tian, I. M. Peters, J. P. Correa-Baena and T. Buonassisi, *Joule*, 2019, **3**, 1437–1451.
100 X. Cai, F. Liu, A. Yu, J. Qin, M. Hatamvand, I. Ahmed, J. Luo, Y. Zhang, H. Zhang and Y. Zhan, *Light: Sci. Appl.*, 2022, 11.
101 J. M. Howard, E. M. Tennyson, B. R. A. Neves and M. S. Leite, *Joule*, 2019, **3**, 325–337.
102 H. K. H. Lee, J. Barbé, S. M. P. Meroni, T. Du, C. Lin, A. Pockett, J. Troughton, S. M. Jain, F. De Rossi and J. Baker, *Solar RRL*, 2019, **3**, 1800207.
103 M. H. Ann, J. Kim, M. Kim, G. Alosaimi, D. Kim, N. Y. Ha, J. Seidel, N. Park, J. S. Yun and J. H. Kim, *Nano Energy*, 2020, **68**, 104321.
104 R. Nie, K. S. Lee, M. Hu, M. J. Paik and S. Il Seok, *Matter*, 2020, **3**, 1701–1713.
105 S. Hwang and T. Yasuda, *Polym. J.*, 2022, 1–20.